Acta Crystallographica Section A
Foundations of Crystallography
ISSN 0108-7673

Received 25 July 2002
Accepted 16 December 2002

A one-dimensional model for small-angle X-ray scattering from crystalline block copolymers

Didier Villers

Laboratoire de Physicochimie des Polymères, Université de Mons-Hainaut, 20 Place du Parc, B-7000 Mons, Belgium. Correspondence e-mail: didier.villers@umh.ac.be

Small-angle X-ray scattering patterns (SAXS) are widely used to study polymers. Quantitative treatment of the intensity curves is often realized to obtain the long period and the linear crystallinity of semicrystalline homopolymers presenting a lamellar morphology, mainly using the correlation function. But even in the one-dimensional case, block copolymer systems exhibit more complicated morphologies that cannot be fully interpreted by this standard method. In this work, a model has been developed based on a previous treatment applicable to systems characterized by two different densities. Two additional densities have been considered to model four phase systems that can occur with block copolymers (*e.g.* two different crystalline domains and amorphous parts). The scattering intensity function was derived as a function of various parameters like the number of stacked lamellar units, the mean values and distributions of widths, and the electron densities.

1. Introduction

Small-angle X-ray scattering patterns (SAXS) are widely used to probe nanoscale structures (1–100 nm) that occur in polymers. This subject has been recently reviewed by Chu & Hsiao (2001). Among the numerous studies, quantitative treatment of the intensity curves is often realized to obtain the long period and the linear crystallinity of semicrystalline homopolymers presenting a lamellar one-dimensional morphology, mainly using the correlation function (Strobl & Schneider, 1980).

Even in the liquid state, block copolymers exhibit complex nanostructures owing to the microphase separation of the blocks at the mesoscopic scale (see Hamley, 1998). Theoretical studies of the equilibrium morphologies are based on the minimization of the free energy for particular geometries, taking into account the block composition in the case of diblock copolymers. Some of the possible structures have cubic, hexagonal or lamellar symmetries. Using SAXS, it has been possible to identify the microdomain morphology of diblock copolymer systems from the relative positions of the scattering maxima. For lamellar phases of liquid diblock copolymers, the SAXS intensity curves can be easily treated like semicrystalline homopolymers, since there are essentially two phases of different electron densities. The correlation functions allow the derivation of the long period together with the lengths of the two components. For some more complicated systems, the number of potential phases is increased and their fine structure can be more complex, *i.e.* by formulating block copolymers with a third block, or when the copolymer contains a crystallizable block. Even in the one-dimensional case, such systems exhibit morphologies that cannot be fully interpreted by a standard method. For example, this is the case of an alternating (multi)block copolymer made of poly(caprolactone) and poly(hexamethylene terephthalate) blocks (PCL–PHT), both being crystallizable (Lefèvre *et al.*, 2001). Combining differential scanning calorimetry (DSC), wide-angle X-ray diffraction (WAXD) and SAXS, they show that PCL and PHT blocks crystallize to form an alternate lamellar structure embedded in an amorphous phase. This corresponds to the following four phases in succession: crystalline PCL – amorphous copolymer – crystalline PHT – amorphous copolymer. A similar behaviour has been observed in a study on poly(ethylene)–poly(ethylethylene) diblock copolymers (PE–PEE) (Ryan *et al.*, 1995), where the four successive phases indicated in the periodic lamellar morphology are: amorphous PE – crystalline PE – amorphous PE – amorphous PEE. In both studies, conclusions have been drawn using peak positions of the SAXS intensity and correlation function curves. Even if misinterpretations are unlikely, a theoretical treatment could be very useful to model the experimental results. Since a one-dimensional two-phase model cannot be used to model these examples, there is a clear need for a more appropriate model which will take into account the periodic succession of four phases that was experimentally proven in these works on block copolymers.

In this work, we present such a model based on the general treatment given by Hosemann (see Hosemann & Bagchi, 1962), initially applied to homopolymers characterized by two different densities (amorphous and crystalline). We have

considered two additional densities to model four phase systems that can occur with block copolymers (*i.e.* the different crystalline domains and amorphous parts that occur in the two mentioned examples). The scattering intensity function was derived as a function of various parameters like the number of stacked lamellar units, the mean values and distributions of phase widths, and the electron densities.

2. The model

Consider a one-dimensional system consisting of N layers numbered j, each made of four successive rods denoted P, Q, R and S. These layers are arranged along an axis u perpendicular to the incident beam $\mathbf{S_0}$, and the electron densities ρ_p, ρ_q, ρ_r and ρ_s are assumed constant in each zone. For simplicity, density differences between the P, Q, R rods and the fourth S rod are used, the density of the latter (ρ_s) is thus supposed to be zero. The rod P having length P_j is so placed that its left end is located at the point u_j and is followed on the right by the rods of length Q_j, R_j and S_j. A schematic view of this model is presented in Fig. 1. These lengths fluctuate across the different layers according to general distribution functions $H_P(P_j)$, $H_Q(Q_j)$, $H_R(R_j)$ and $H_S(S_j)$, respectively. We assume also that there is no correlation between any of these length. These assumptions are sufficient to determine the total scattering intensity as a function of the reciprocal coordinate s.

3. Mathematical development

Following the previous assumptions, the amplitude of the scattered radiation is given by

$$a(s) = \int_{u_1}^{u_{N+1}} \rho(u) \exp(-2\pi i s u)\, \mathrm{d}u. \tag{1}$$

Since $\rho_s = 0$, the amplitude of the N layers is expressed as $3N$ terms:

$$\begin{aligned} a(s) = \sum_{j=1}^{N} & \int_0^{P_j} \rho_p \exp[-2\pi i s(u_j + p)]\, \mathrm{d}p \\ & + \int_0^{Q_j} \rho_q \exp[-2\pi i s(u_j + P_j + q)]\, \mathrm{d}q \\ & + \int_0^{R_j} \rho_r \exp[-2\pi i s(u_j + P_j + Q_j + r)]\, \mathrm{d}r. \end{aligned} \tag{2}$$

Integrals on p, q and r can easily be solved:

$$\begin{aligned} a(s) = (1/2\pi i s) \sum_{j=1}^{N} & \exp(-2\pi i s u_j)\big\{\rho_p[1 - \exp(-2\pi i s P_j)] \\ & + \rho_q \exp(-2\pi i s P_j)[1 - \exp(-2\pi i s Q_j)] \\ & + \rho_r \exp[-2\pi i s(P_j + Q_j)][1 - \exp(-2\pi i s R_j)]\big\}. \end{aligned} \tag{3}$$

The resulting intensity will therefore be

$$\begin{aligned} I(s) &= a(s)a^*(s) \\ &= [1/(2\pi s)^2] \sum_{j=1}^{N} \sum_{k=1}^{N} \exp[-2\pi i s(u_j - u_k)] \\ &\quad \times \big\{\rho_p[1 - \exp(-2\pi i s P_j)] + \rho_q \exp(-2\pi i s P_j) \\ &\quad \times [1 - \exp(-2\pi i s Q_j)] + \rho_r \exp[-2\pi i s(P_j + Q_j)] \\ &\quad \times [1 - \exp(-2\pi i s R_j)]\big\}\big\{\rho_p[1 - \exp(2\pi i s P_k)] \\ &\quad + \rho_q \exp(2\pi i s P_k)[1 - \exp(2\pi i s Q_k)] \\ &\quad + \rho_r \exp[2\pi i s(P_k + Q_k)][1 - \exp(2\pi i s R_k)]\big\}. \end{aligned} \tag{4}$$

This double summation can be evaluated by considering the terms in groups: the N diagonal ones with $j = k$, the $2(N-1)$ terms with $j = k-1$ and $j = k+1$, the $2(N-2)$ terms with $j = k-2$ and $j = k+2$, ...

3.1. Diagonal terms

The terms for which $j = k$ can be reorganized as a summation of 6 terms:

$$\begin{aligned} & [1/(2\pi s)^2] \sum_{j=1}^{N} \rho_p^2[1 - \exp(-2\pi i s P_j)][1 - \exp(2\pi i s P_j)] \\ & \quad + \rho_q^2[1 - \exp(-2\pi i s Q_j)][1 - \exp(2\pi i s Q_j)] \\ & \quad + \rho_r^2[1 - \exp(-2\pi i s R_j)][1 - \exp(2\pi i s R_j)] \\ & \quad + \rho_p\rho_q\big\{[\exp(2\pi i s P_j) - 1][1 - \exp(2\pi i s Q_j)] \\ & \quad + [\exp(-2\pi i s P_j) - 1][1 - \exp(-2\pi i s Q_j)]\big\} \\ & \quad + \rho_p\rho_r\big(\{\exp[2\pi i s(P_j + Q_j)] - \exp(2\pi i s Q_j)\} \\ & \quad \times [1 - \exp(2\pi i s R_j)] + \{\exp[-2\pi i s(P_j + Q_j)] \\ & \quad - \exp(-2\pi i s Q_j)\}[1 - \exp(-2\pi i s R_j)]\big) + \rho_q\rho_r\big\{\exp(2\pi i s Q_j) \\ & \quad \times [1 - \exp(-2\pi i s Q_j)][1 - \exp(2\pi i s R_j)] + \exp(-2\pi i s Q_j) \\ & \quad \times [1 - \exp(2\pi i s Q_j)][1 - \exp(-2\pi i s R_j)]\big\}. \end{aligned} \tag{5}$$

The possible values P_j, Q_j and R_j are given statistically by the distributions $H_P(P_j)$, $H_Q(Q_j)$ and $H_R(R_j)$. All values from 0 to ∞ must be considered for the evaluation of I. Since H are defined as distributions, we have:

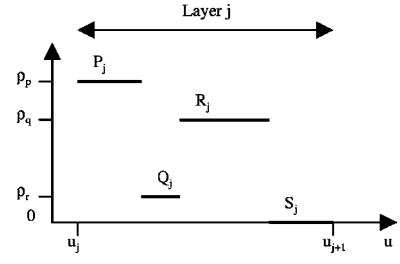

Figure 1
Schematic description of the successive layers in the model.

$$\int_0^\infty H_P \,\mathrm{d}P_j = 1$$
$$\int_0^\infty H_Q \,\mathrm{d}Q_j = 1 \qquad (6)$$
$$\int_0^\infty H_R \,\mathrm{d}R_j = 1.$$

The following integrals, which are in fact Fourier transforms of the distribution, are introduced:

$$F_P = \int_0^\infty H_P \exp(-2\pi i s P_j)\,\mathrm{d}P_j$$
$$F_Q = \int_0^\infty H_Q \exp(-2\pi i s Q_j)\,\mathrm{d}Q_j \qquad (7)$$
$$F_R = \int_0^\infty H_R \exp(-2\pi i s R_j)\,\mathrm{d}R_j.$$

All the N diagonal terms are identical, and (5) becomes

$$\begin{aligned}[N/(2\pi s)^2]\big\{&\rho_p^2(2 - F_P - F_P^*) + \rho_q^2(2 - F_Q - F_Q^*)\\ &+ \rho_R^2(2 - F_R - F_R^*) + \rho_p\rho_q(F_P^* + F_Q^* - F_P^*F_Q^* - 1 + F_P + F_Q\\ &- F_PF_Q - 1) + \rho_p\rho_r[F_Q^*(F_P^* + F_R^* - F_P^*F_R^* - 1)\\ &+ F_Q(F_P + F_R - F_PF_R - 1)] + \rho_q\rho_r(F_Q^* + F_R^* - F_Q^*F_R^* - 1\\ &+ F_Q + F_R - F_QF_R - 1)\big\}. \end{aligned} \qquad (8)$$

The superscript * denotes the complex conjugates of the corresponding functions. Sums of complex conjugate pairs $Z^* + Z$ can be substituted by $2\mathrm{Re}\{Z\}$ (Re{} denotes the real part), which yields

$$\begin{aligned}[2N/(2\pi s)^2][&\rho_p^2\mathrm{Re}\{1 - F_P\} + \rho_q^2\mathrm{Re}\{1 - F_Q\} + \rho_r^2\mathrm{Re}\{1 - F_R\}\\ &+ \rho_p\rho_q\mathrm{Re}\{1 + F_PF_Q - F_P - F_Q\}\\ &+ \rho_p\rho_r\mathrm{Re}\{(1 + F_PF_R - F_P - F_R)F_Q\}\\ &+ \rho_q\rho_r\mathrm{Re}\{1 + F_QF_R - F_Q - F_R\}]. \end{aligned} \qquad (9)$$

3.2. Terms with $j = k - 1$ and $j = k + 1$

Let us firstly consider terms where $j = k - 1$ or $k = j + 1$. In this case, we have

$$\exp[-2\pi i s(u_j - u_k)] = \exp[2\pi i s(P_j + Q_j + R_j + S_j)]$$

and the corresponding sum is

$$\begin{aligned}[1/(2\pi s)^2] \sum_{j=1}^{N-1} &\exp[2\pi i s(P_j + Q_j + R_j + S_j)]\\ &\times \Big(\rho_p^2[1 - \exp(-2\pi i s P_j)][1 - \exp(-2\pi i s P_{j+1})]\\ &+ \rho_q^2\exp(-2\pi i s P_j)[1 - \exp(-2\pi i s Q_j)]\exp(2\pi i s P_{j+1})\\ &\times [1 - \exp(-2\pi i s Q_{j+1})] + \rho_r^2\exp[-2\pi i s(P_j + Q_j)]\\ &\times [1 - \exp(-2\pi i s R_j)]\exp[2\pi i s(P_{j+1} + Q_{j+1})]\\ &\times [1 - \exp(-2\pi i s R_{j+1})] + \rho_p\rho_q\big\{[1 - \exp(-2\pi i s P_j)]\\ &\times \exp(2\pi i s P_{j+1})[1 - \exp(2\pi i s Q_{j+1})] + [1 - \exp(2\pi i s P_{j+1})]\\ &\times \exp(-2\pi i s P_j)[1 - \exp(-2\pi i s Q_j)]\big\}\\ &+ \rho_p\rho_r\big\{[1 - \exp(-2\pi i s P_j)]\exp[2\pi i s(P_{j+1} + Q_{j+1})]\\ &\times [1 - \exp(2\pi i s R_{j+1})] + [1 - \exp(2\pi i s P_{j+1})]\\ &\times \exp[-2\pi i s(P_j + Q_j)][1 - \exp(-2\pi i s R_j)]\big\}\\ &+ \rho_q\rho_r\big\{[1 - \exp(-2\pi i s P_j)][1 - \exp(-2\pi i s Q_j)]\\ &\times \exp[2\pi i s(P_{j+1} + Q_{j+1})][1 - \exp(2\pi i s R_{j+1})]\\ &+ \exp(2\pi i s P_{j+1})[1 - \exp(2\pi i s Q_{j+1})]\exp[-2\pi i s(P_j + Q_j)]\\ &\times [1 - \exp(-2\pi i s R_j)]\big\}\Big). \end{aligned} \qquad (10)$$

As in the previous section, we have to consider the following integrals and definitions:

$$\int_0^\infty H_S \,\mathrm{d}S_j = 1 \quad \text{and} \quad F_S = \int_0^\infty H_S \exp(-2\pi i s S_j)\,\mathrm{d}S_j \qquad (11)$$

and (10) becomes

$$\begin{aligned}[(N-1)/(2\pi s)^2]\big[&-\rho_p^2F_Q^*F_R^*F_S^*(1 - F_P^*)^2 - \rho_q^2F_P^*F_R^*F_S^*(1 - F_Q^*)^2\\ &- \rho_R^2F_P^*F_Q^*F_S^*(1 - F_R^*)^2 - \rho_p\rho_qF_R^*F_S^*(1 - F_P^*)(1 - F_Q^*)\\ &\times (F_P^*F_Q^* + 1) - \rho_p\rho_rF_S^*(1 - F_P^*)(1 - F_R^*)(F_P^*F_Q^{*2}F_R^* + 1)\\ &- \rho_q\rho_rF_P^*F_S^*(1 - F_R^*)(1 - F_Q^*)(F_Q^*F_R^* + 1)\big]. \end{aligned} \qquad (12)$$

The contribution of the $j = k + 1$ terms is the complex conjugate of this last expression.

3.3. Other off-diagonal terms

The next group of terms is such that $j = k - 2$ or $j = k + 2$. This yields firstly to an equation analogous to (10) beginning with

$$\begin{aligned}[1/(2\pi s)^2] \sum_{j=1}^{N-2} &\exp[2\pi i s(P_j + Q_j + R_j + S_j + P_{j+1} + Q_{j+1} + R_{j+1}\\ &+ S_{j+1})]\big\{\rho_p^2[1 - \exp(-2\pi i s P_j)][1 - \exp(-2\pi i s P_{j+2})]\ldots. \end{aligned} \qquad (13)$$

These terms can also be rewritten as

$$[(N-2)/(2\pi s)^2]\big[-\rho_p^2F_Q^*F_R^*F_S^*(F_P^*F_Q^*F_R^*F_S^*)(1 - F_P^*)^2 - \rho_q^2\ldots. \qquad (14)$$

Comparing this to (12), we observe the presence of the constant factor $(F_P^*F_Q^*F_R^*F_S^*)$. All subsequent off-diagonal terms such that $j = k - r$ are similar, with factors of the general form $(F_P^*F_Q^*F_R^*F_S^*)^r$. We have also complex-conjugate contributions from terms such that $j = k + r$.

3.4. Final expression of the intensity

All the terms are added to give

$$
\begin{aligned}
I(s) = [2N/(2\pi s)^2]\big[&\rho_p^2 \mathrm{Re}\{1 - F_P\} + \rho_q^2 \mathrm{Re}\{1 - F_Q\} \\
&+ \rho_r^2 \mathrm{Re}\{1 - F_R\} + \rho_p\rho_q \mathrm{Re}\{1 + F_P F_Q - F_P - F_Q\} \\
&+ \rho_p\rho_r \mathrm{Re}\{(1 + F_P F_R - F_P - F_R)F_Q\} \\
&+ \rho_q\rho_r \mathrm{Re}\{1 + F_Q F_R - F_Q - F_R\}\big] \\
&- 2\mathrm{Re}\Big\{\Big[\sum_{r=0}^{N-1} (F_P F_Q F_R F_S)^r (N - r - 1)\Big] \\
&\times \big[\rho_p^2 F_Q F_R F_S (1 - F_P)^2 + \rho_q^2 F_P F_R F_S (1 - F_Q)^2 \\
&+ \rho_r^2 F_P F_Q F_S (1 - F_R)^2 + \rho_p\rho_q F_R F_S (1 - F_P)(1 - F_Q) \\
&\times (1 + F_P F_Q) + \rho_p\rho_r F_S (1 - F_P)(1 - F_R)(1 + F_P F_Q^2 F_R) \\
&+ \rho_q\rho_r F_P F_S (1 - F_R)(1 - F_Q)(1 + F_Q F_R)\big]\Big\}. \qquad (15)
\end{aligned}
$$

As the values of the distribution functions are always less than unity, the following summation rules converge and can be applied (q represents any product of distribution functions):

$$\sum_{r=0}^{N-1} q^r = \frac{1 - q^N}{1 - q} \qquad (16)$$

$$\sum_{r=0}^{N-1} (r+1) q^r = \frac{\mathrm{d}}{\mathrm{d}q}\Big(q \sum_{r=0}^{N-1} q^r\Big) = \frac{1 - q^N}{(1-q)^2} - N\frac{q^N}{1-q} \qquad (17)$$

$$
\begin{aligned}
\sum_{r=0}^{N-1} q^r (N - r - 1) &= N\frac{1 - q^N}{1 - q} - \frac{1 - q^N}{(1-q)^2} + N\frac{q^N}{1-q} \\
&= \frac{N}{1-q} - \frac{1 - q^N}{(1-q)^2}. \qquad (18)
\end{aligned}
$$

The result is presented as the sum of two intensity terms: $I = I_B + I_C$, where

$$
\begin{aligned}
I_B(s) = (N/2\pi^2 s^2)\mathrm{Re}\big\{&(1 - F_P F_Q F_R F_S)^{-1}\big[\rho_p^2 (1 - F_P) \\
&\times (1 - F_Q F_R F_S) + \rho_q^2 (1 - F_Q)(1 - F_P F_R F_S) \\
&+ \rho_r^2 (1 - F_R)(1 - F_P F_Q F_S) \\
&- \rho_p\rho_q (1 - F_P)(1 - F_Q)(1 + F_R F_S) \\
&- \rho_p\rho_r (1 - F_P)(1 - F_R)(F_Q + F_S) \\
&- \rho_q\rho_r (1 - F_Q)(1 - F_R)(1 + F_P F_S)\big]\big\} \qquad (19)
\end{aligned}
$$

and

$$
\begin{aligned}
I_C(s) = \frac{1}{2\pi^2 s^2}\mathrm{Re}\Big\{&\frac{1 - (F_P F_Q F_R F_S)^N}{(1 - F_P F_Q F_R F_S)^2}\big[\rho_p^2 F_Q F_R F_S (1 - F_P)^2 \\
&+ \rho_q^2 F_P F_R F_S (1 - F_Q)^2 + \rho_r^2 F_P F_Q F_S (1 - F_R)^2 \\
&+ \rho_p\rho_q F_R F_S (1 - F_P)(1 - F_Q)(1 + F_P F_Q) \\
&+ \rho_p\rho_r F_S (1 - F_P)(1 - F_R)(1 + F_P F_Q^2 F_R) \\
&+ \rho_q\rho_r F_P F_S (1 - F_Q)(1 - F_R)(1 + F_Q F_R)\big]\Big\}. \qquad (20)
\end{aligned}
$$

I_B is directly proportional to N whereas I_C gives the zero-order scatter which can be neglected if N is sufficiently large and if the distribution functions are sufficiently broad (a condition generaly fulfilled with polymers). From these expressions, it is possible to obtain as a particular case the intensity terms for the analogous two-phase (Y, Z) classical model (Hosemann & Bagchi, 1962), using the following assumptions:

$$
\begin{aligned}
&\rho_q = \rho_z = 0 \\
&\rho_p = \rho_r = \rho_y = \rho \\
&F_P = F_R = F_Y \\
&F_Q = F_S = F_Z.
\end{aligned} \qquad (21)
$$

Then,

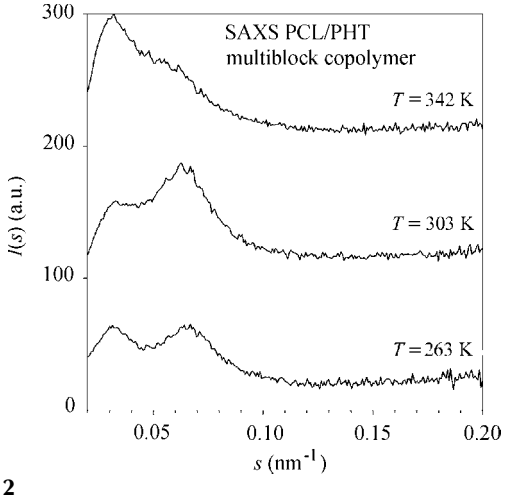

Figure 2
Experimental SAXS profiles of a PCL–PHT copolymer taken at three temperatures (263, 303 and 342 K).

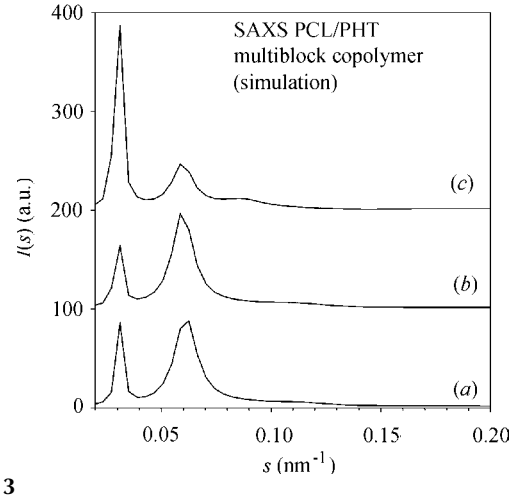

Figure 3
Simulated SAXS profiles of a PCL–PHT copolymer. $\rho_p = 0.6$ (crystalline PCL), $\rho_q = \rho_s = 0$ (amorphous PCL–PHT), $\rho_r = 1$ (crystalline PHT). (*a*) P = 4.8 nm, Q = 10.2 nm, R = 7 nm, S = 10.2 nm. (*b*) Same parameters as (*a*) except $Q = S$ = 10.6 nm. (*c*) Fusion of PCL zones: same parameters as (*b*), except $\rho_p = 0$.

$$I_B(s) = \frac{2N\rho^2}{2\pi^2 s^2}\,\mathrm{Re}\left\{\frac{(1-F_Y)(1-F_Z)}{1-F_YF_Z}\right\} \quad (22)$$

$$I_C(s) = \frac{\rho^2}{2\pi^2 s^2}\,\mathrm{Re}\left\{F_Z\left(\frac{1-F_Y}{1-F_YF_Z}\right)^2[1-(F_YF_Z)^{2N}]\right\}. \quad (23)$$

4. Applications

For samples of semicrystalline block copolymers, the main term of interest in the scattered intensity is I_B. Therefore, (19) has been evaluated for the two particular cases mentioned in the *Introduction*. In this equation, densities explicitly appear whereas the thicknesses and their distributions H are introduced *via* (7) and (11), which allow computation of the functions F.

4.1. PCL–PHT alternating block copolymer

The melting of this copolymer was studied by SAXS using synchrotron radiation (Lefèvre *et al.*, 2001). Intensity curves taken at three different temperatures (263, 303 and 342 K) are shown in Fig. 2. It has been concluded from wide-angle X-ray diffraction, differential calorimetry, SAXS and chemical considerations that the system consists of crystalline lamellae of PCL and PHT embedded in amorphous parts. Only the temperature (and consequently the densities) are changed between the first two measurements whereas the PCL crystalline phase has been melted at 342 K. The experimental SAXS curves show that the area of the second peak is markedly increased at 303 K and that the melting of PCL gives the almost entire disappearance of this second peak. Fig. 3 shows that the same observations can be made on the simulated profiles which have been computed using parameters suggested from the mentioned study: density values of 1.17 for crystalline PCL, 1.20 for crystalline PHT and 1.12 for the amorphous copolymer. The change between 263 and 303 K has been obtained by changing the amorphous thickness $Q = S$ from 10.2 to 10.6 nm, a change compatible with the important thermal expansion of the amorphous parts. Simulation of the curve at 342 K has been obtained by superseding the density of PCL by zero, which corresponds to a crystal-to-amorphous transition. These simulations agree with the morphological evolution experimentally observed.

4.2. PE–PEE block copolymer

Ryan *et al.* (1995) have studied the morphology of PE–PEE diblocks quenched from lamellar microphase-separated phases below the PE crystallization temperature. In such conditions, the lamellar morphology can be interpreted as the repeated succession of the four following phases: amorphous PE, crystalline PE, amorphous PE and amorphous PEE. Fig. 4 shows the SAXS intensity profile, characterized by four peaks of decreasing intensity. The authors have used the scattering density correlation function to assess the four domain thicknesses. From the positions of peak maxima and minima (at 4.7, 15.3, 22.3 and 32.4 nm), they propose the values for the thicknesses of the four phases mentioned before: 5.3, 4.7, 5.3 and 17.1 nm. These findings have been reinforced with the mathematical model developed in the present paper. Indeed, it has been possible to simulate a SAXS profile similar to the experimental one, using very close thicknesses with differences less than 5% (P = 5.2, Q = 4.9, R = 5.2, S = 17.8 nm) (see Fig. 5).

5. Conclusions

The main topic of this paper was to develop a one-dimensional mathematical model to model four phase systems that can occur with block copolymers. This model has been applied to two selected experimental studies. It has been shown that the complex SAXS patterns observed in such block copolymer systems can be simulated on a theoretical basis, using only a

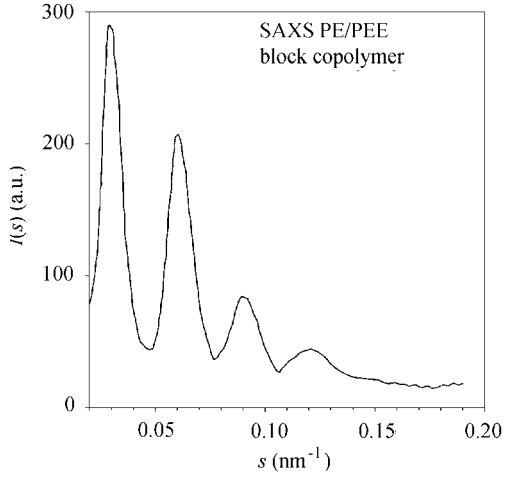

Figure 4
Experimental SAXS profile of a PE–PEE copolymer exhibiting a lamellar morphology.

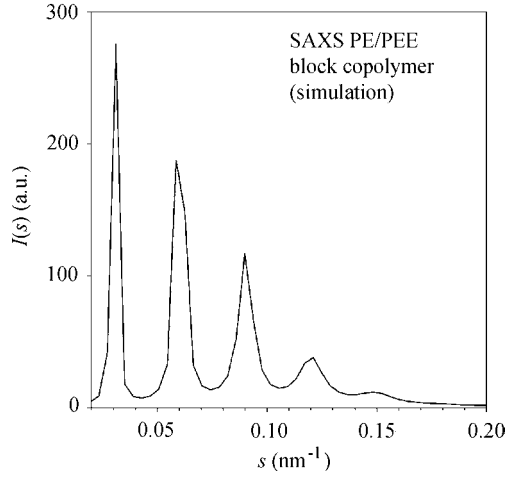

Figure 5
Simulated SAXS profile of a PE–PEE copolymer. P = 5.2 nm (amorphous PE), Q = 4.9 nm (crystalline PE), R = 5.2 nm (amorphous PE), S = 17.8 nm (amorphous PEE), $\rho_p = \rho_r = 0.005$, $\rho_q = 1$.

few parameters having direct physical meaning to describe the morphologies: the mean thicknesses, their distributions and the densities. Starting from this study and combining it with non-linear least-squares numerical methods, it would be possible to analyse scattering data in order to extract morphological parameters, but this approach is beyond the scope of the present paper.

The author thanks Dr P. Damman for fruitful discussions.

References

Chu, B. & Hsiao, B. S. (2001). *Chem. Rev.* **101**, 1727–1761.
Hamley, I. W. (1998). *The Physics of Block Copolymers*. Oxford University Press.
Hosemann, R. & Bagchi, S. N. (1962). *Direct Analysis of Diffraction by Matter*, pp. 408–413. Amsterdam: North-Holland.
Lefèvre, C., Villers, D., Koch, M. H. J. & David, C. (2001). *Polymer*, **42**, 8769–8777.
Ryan, A. J., Hamley, I. W., Bras, W. & Bates, F. S. (1995). *Macromolecules*, **28**, 3860–3868.
Strobl, G. R. & Schneider, M. J. (1980). *J. Polym. Sci. Polym. Phys. Ed.* **18**, 1343–1359.